Seasonal regimes of daily precipitation in Iran

Tayeb Raziei[1], Abbas Mofidi[2], João A. Santos[3] and Isabella Bordi[4]

[1] *Research Institute for Water Scarcity and Drought in Agriculture and Natural Resources (RIWSD), Tehran, Iran, E-mail: tayebrazi@scwmri.ac.ir*

[2] *Department of Geography, Ferdowsi University of Mashhad, Mashhad, Iran, E-mail: abbasmofidi@um.ac.ir*

[3] *Centre for the Research and Technology of Agro- Environment and Biological Sciences (CITAB), UTAD, Portugal, E-mail: santos@utad.pt*

[4] *Department of Physics, Sapienza University of Rome, Rome, Italy, E-mail: isabella.bordi@roma1.infn.it*

Abstract

Seasonal regimes of daily precipitation over Iran and their associations to large-scale atmospheric circulation types are assessed using APHRODITE gridded daily precipitation dataset covering period 1961–2004. Regional modes of daily precipitation variability for each season (excluding summer),were isolated separately by applying a PCA with Varimax rotation, to the subset of days when at least 10% of all selected grid-points over Iran recorded precipitation amounts above 5 mm. To characterize the dynamical features associated with each precipitation regime, composites of daily atmospheric fields are computed by only averaging days characterized by a strong positive phase in the rotated PC (scores above 1.5). In autumn and winter, Iran is divided into five precipitation regimes. In spring, only four precipitation regimes are identified. The analysis of the composites suggests that the spatial distribution of precipitation over Iran is largely governed by the geographical position of two synoptic systems: the mid-tropospheric trough over the Middle East and the Arabian anticyclone. It is shown that in almost all precipitation regimes, the trough, as a pre-conditioning factor, leads to regional-scale ascending motions, whereas the Arabian anticyclone induce low-tropospheric moisture transports from the southern water bodies into the cyclonic systems nearby Iran.

Introduction

Space-time variability of precipitation in a region plays an essential role in water resource management, motivating many research efforts to identify large-scale atmospheric circulation types (CTs) leading to precipitation events and their effects on the frequency and amount of precipitation (e.g. Corte-Real et al., 1998; Romero et al., 1999 and references therein). In Iran, precipitation variability is mainly controlled by the complex orography that enhance (mitigate) precipitation associated with large-scale CTs on their windward (leeward) side. Several authors have analysed drought phenomenon in Iran (Morid et al., 2006; Raziei et al., 2008, 2009), the possible link between atmospheric indices and surface climate variables (Nazemosadat and Cordery, 2000; Nazemosadat and Ghasemi, 2004; Ghasemi and Khalili, 2006; Raziei et al., 2009), or trends in extreme precipitation events (Rahimzadeh et al., 2009; Zhang et al., 2005). However, rare attempts have been devoted to the relationship between large-scale CTs and daily precipitation. Recently, CTs for the Middle East have been identified and their impact on the occurrence of winter dry/wet spells in western Iran were investigated (Raziei et al., 2011). Here we complement that study by identifying the spatial patterns of seasonal daily precipitation variability over Iran and their association to large-scale CTs.

Data and Methods

Data: Analysis refers to autumn (SON), winter (DJF) and spring (MAM) which well represents the rainy seasons in all parts of Iran. Summer is excluded, since it is, on average, extremely dry in almost all of the country, owing to the dominant subtropical high pressure system that induces strong subsidence and resulting stable weather conditions. Daily precipitation data have been retrieved from the Asian Precipitation-Highly-Resolved Observational Data Integration Towards Evaluation of the Water Resources (APHRODITE) project for the Middle East (Yatagai et al., 2009); the new release V0902 with a spatial resolution of 0.5 was used.

Daily mean of 500 hPa geopotential height and daily means of specific humidity, zonal (U) and meridional (V) wind components at 850 hPa and mean sea level pressure for all considered seasons, covering Iran and the Middle East sector (10°E–80°E, 10°N–60°N), with a 2.5° latitude-longitude resolution, were retrieved from NCEP/NCAR reanalysis (Kalnay *et al.*, 1996).

Methods: For each considered season a Principal Component Analysis (PCA) with Varimax rotation has been separately applied to to the subset of days when at least 10% of all selected grid-points over Iran recorded precipitation amounts above 5 mm. However, since some assumptions in PCA require normally distributed variables (Fovell and Fovell, 1993), the log10-transformation is applied to daily precipitation prior to PCA; zero values are replaced by 0.01 before taking logarithms (Romero et al., 1999; Neal and Phillips, 2009). This transformation significantly reduces the positive skewness of the empirical distributions, yielding their convergence to normality. Therefore, the S-mode PCA with Varimax rotation was separately applied to the log10-transformed precipitation time series for SON, DJF and MAM. The initial data matrices used as inputs for PCA consist of 638×684, 638×976, 638×721 (variables × cases) for SON, DJF and MAM, respectively; variables are the selected grid points over Iran (638) and cases correspond to days when at least 10% of all grid points have precipitation totals ≥ 5 mm. According to the North's rule-of-thumb, (North et al., 1982), only the first five (four) orthogonal modes for SON and DJF (MAM) are "well-defined" (i.e. non-degenerated) at a 95% confidence level and are then retained for subsequent rotation.

In order to analyze the connection between the seasonal regimes of daily precipitation and the driving large-scale atmospheric circulation types, a compositing methodology is applied (Yarnal et al., 2001). Composites of Z500 and respective relative vorticity, of the 850 hPa moisture transport and corresponding streamlines are computed for each considered season and for each precipitation mode, by only taking into account days with RPC ≥ 1.5 (strong positive phase). These variables jointly provide a detailed description of the main dynamical features associated with a precipitation regime.

Results

Spatial patterns and seasonal regimes of daily precipitation

Figure 1 displays the rotated empirical orthogonal functions (REOFs) of daily precipitation for SON, DJF and MAM, ranked according to their similarity rather than to their eigenvalues. Figure 1a–e shows the five REOFs of daily precipitation for SON. As can be noted the country is divided into five sub-regions, each one characterized by high positive loadings. The first and second REOFs represent 14.0% and 13.8% of total variance, respectively, and isolate central-western and south-western Iran as distinct sub-regions of daily precipitation variability. REOF 3 explains 13.1% of total variance and isolates a sub-region in north-eastern Iran. Independent precipitation variability in south-eastern and north-western Iran is represented by REOF 4 and 5, respectively (11.4% and 6.9% of total variance). In DJF, the target area is also divided into five sub-regions of precipitation variability very similar to those previously identified for SON (Fig. 2f–j). In MAM, the four REOFs also show similar sub-regions, but now the central-western and north-western regions are jointly represented by the first mode (Fig. 2k–n). The Varimax rotation allows the identification of areas with largely independent climate variability, as the rotated PC scores (RPCs) are temporally orthogonal (Rencher, 1998). However, the orthogonality of RPCs does not guarantee the existence of different precipitation regimes in the sub-regions. A way to objectively describe a precipitation regime is the analysis of the empirical distribution of daily precipitation totals in the area of interest. Thus, in order to test if the identified sub-regions are characterized by different precipitation regimes, the statistical distributions of area-mean daily precipitation, averaged over grid points with REOF loadings ≥ 0.6, are considered (Fig. 1). The two-sample Kolmogorov-Smirnov test is applied to check the null-hypothesis that the distributions are equal. According to the hypothesis testing, all sub-regions are characterized by non-equal distributions, at least at a 99% confidence level ($p < 0.01$), which suggests that their own precipitation regimes are very likely to be different.

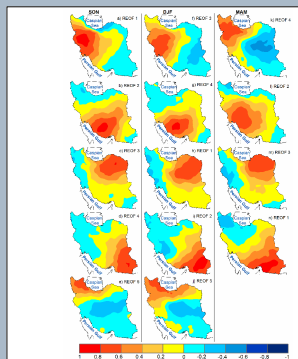

Figure 1: Leading REOFs of daily precipitation over Iran for SON (a-e), DJF (f-j) and MAM (k-n).

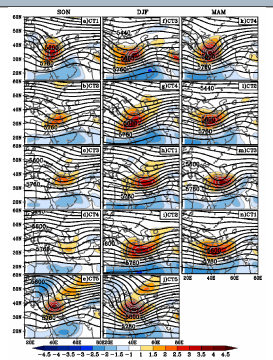

Figure 2: Circulation types (CTs): Composites of the 500 hPa geopotential height (contours in gpm) and 500 hPa relative vorticity (shading in 10^{-5} s^{-1}) associated with the precipitation regimes in SON (a–e), DJF (f–j) and MAM (k–n).

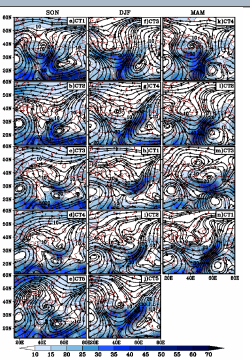

Figure 3: Circulation types (CTs): Composite maps of moisture transport (g s−1) and streamlines at 850 hPa associated with the precipitation regimes in SON (a–e), DJF (f–j) and MAM (k–n).

Precipitation regimes and large-scale atmospheric circulation types

Central-western regime: For SON, the presence of a deep mid-tropospheric trough westwards of Iran (Fig. 2a) in accompanying with a cyclone north-westwards of Iraq and the Arabian anticyclone southwards (Fig. 3a) is highly favourable to precipitation occurrences in central-western Iran. The CTs for DJF (Fig. 2f) and MAM (Fig. 2k) are very similar to the corresponding SON pattern, but with a shift in the position of the trough and ridge axis.

South-western regime: In SON, this regime is associated with a relatively weak trough over Iraq (Fig. 2b) and the Arabian anticyclone in eastern Saudi Arabia (Fig. 3b), favouring moisture transports into southern Iran. The 500 hPa CT for DJF (Fig. 2g) is similar to its autumn counterpart (Fig. 2b), especially considering the flow curvature over the area, but they differ in the geopotential gradient. For MAM the 500 hPa CT shows a wide trough over Syria and Jordan and a ridge over eastern Iran (Fig. 2l), while the Arabian anticyclone induces moisture transports from the southern water bodies to western Iran, (Fig.3l).

North-eastern regime: In SON, this regime is related to a trough with its axis over the Caspian Sea (Fig. 2c) which is accompanied by a low-tropospheric anticyclonic circulation southwards of Iran (Fig. 3c) , enabling the incursion of moisture transports into eastern Iran. In DJF, the 500 hPa CT (Fig. 2h) is similar to the corresponding SON pattern (Fig. 2c), but the main trough is now southwardly displaced and the positive vorticity area is much wider and stronger. For MAM, a trough over western Iran (Fig. 2m) is connected in the lower level to a cyclonic system in north-eastern Iran and to the Arabian anticyclone (Fig. 3m).

South-eastern regime: In SON, this regime is characterized by a weak trough over Iran in upper level (Fig. 2d) and a cyclonic circulation over Iran and the Arabian anticyclone in the lower level (Fig. 3d), leading to moisture transport and precipitation occurrence over the regions. In DJF, the 500 hPa CT is characterized by a trough in western Iran (Fig. 2i) and a convergence of moisture transports over south-eastern Iran (Fig. 3i). In MAM, the 500 hPa CT features a wide trough, with associated positive vorticity over Iraq and western Iran (Fig. 2n) and the Arabian anticyclone over the Arabian Sea (Fig. 3n).

North-western (Caspian Sea) regime: In SON, this regime is characterized with a deep trough extending from eastern Turkey towards the Caspian Sea (Fig.2e) and a strong anticyclone located between the Black Sea and the Caspian Sea (Fig. 3e), resulting in precipitation occurrence over the area. In DJF, the mid- and low-tropospheric CTs for this regime (Fig. 2j and 3j) are very similar to their autumn counterparts, though in winter the trough is deeper than in autumn and southwardly displaced. In MAM, this regime is absent since the central-western and north-western regimes are jointly represented by fourth REOF (Fig. 1k).

Summary

In autumn and winter, Iran is divided into five precipitation regimes, with their corresponding modes cumulatively accounting for about 59% of total variance; in spring, four precipitation regimes (55% of variance) are identified. The study suggests that the spatial distribution of precipitation over Iran is mainly governed by large-scale circulation types and, in particular, by the geographical position of the mid-tropospheric troughs/ridges and of the low-tropospheric Arabian anticyclone. The trough, as a pre-conditioning factor, can provide regional scale ascending motions, whilst the Arabian anticyclone can transport moisture from southern water bodies into the cyclonic systems. Precipitation occurrence over western Iran is particularly favoured when a trough extends over the eastern Mediterranean to Iraq, whereas precipitation is very likely to occur in the eastern half of the country when a trough and a ridge are located over western Iran and Pakistan, respectively. The present results suggest that a few CTs contribute to the occurrence of most of the precipitation events in the identified sub-regions. However, the rain-generating CTs differ from one season to the other, even if some common features are detectable.

References

Corte-Real, J., Qian, B., Xu, H., 1998: Regional climate change in Portugal: precipitation variability associated with large-scale atmospheric circulation. *Int. J. Climatol.*, 18, 619–635.

Fovell, R.G., Fovell, M.Y., 1993: Climate zones of the conterminous United States defined using cluster analysis. J. Climate, 6, 2103–2135.

Ghasemi, A.R., Khalili, D., 2006: The influence of the Arctic Oscillation on winter temperatures in Iran. *Theor. Appl. Climatol.*, **85**, 149–164.

Morid, S., Smakhtin, V., Moghaddasi, M., 2006: Comparison of seven meteorological indices for drought monitoring in Iran. *Int. J. Climatol.*, 26, 971–985.

Nazemosadat, M.J., Cordery, I., 2000: On the relationships between ENSO and autumn rainfall in Iran. Int. J. Climatol., 20, 47-61.

Nazemosadat, M.J., Ghasemi, A.R., 2004: Quantifying the ENSO-related shifts in the intensity and probability of drought and wet periods in Iran. J. Climate, 17, 4005-4018.

Neal, R.A., Phillips, I.D., 2009: Summer daily precipitation variability over the East Anglian region of Great Britain. *Int. J. Climatol.*, 29, 1661–1679.

North, G.R., Bell, T.L., and Cahalan, R.F., 1982: Sampling errors in the estimation of empirical orthogonal functions. *Mon. Wea. Rev.*, 110, 699–706.

Kalnay, E., and coauthors, 1996: The NCEP/NCAR 40-year reanalysis project. *Bull. Amer. Meteor. Soc.*, 77, 437–471.

Rahimzadeh, F., Asgari, A., Fattahi, E., 2009: Variability of extreme temperature and precipitation in Iran during recent decades. *Int. J. Climatol.*, 29, 329–343.

Raziei, T., Bordi, I., Pereira, L.S., 2008: A precipitation-based regionalization for Western Iran and regional drought variability. *Hydrol. Earth Syst. Sci.*, 12, 1309–1321.

Raziei, T., Saghafian, B., Paulo, A.A., Pereira, L.S., Bordi, I., 2009: Spatial patterns and temporal variability of drought in western Iran. *Water Resour. Manage.*, 23, 439–455.

Raziei, T., Bordi, I., Pereira, L.S., Corte-Real, J., Santos, J.A., 2011: Relationship between daily atmospheric circulation patterns and winter dry/wet spells in western Iran, *Int. J. Climatol.*, Submitted.

Richman, M.B., Lamb, P.J., 1987: Pattern analysis of growing season precipitation in southern Canada. Atmosphere-Ocean, 25, 137–158.

Romero, R., Sumner, G., Ramis, C., Genoves, C., 1999: A classification of the atmospheric circulation patterns producing significant daily rainfall in the Spanish Mediterranean area. *Int. J. Climatol.*, 19, 765–785.

Yatagai, A., O. Arakawa, K. Kamiguchi, H. Kawamoto, M. I. Nodzu, A. Hamada, 2009: A 44-year daily gridded precipitation dataset for Asia based on a dense network of rain gauges. *SOLA*, 5, 137–140.

Yarnal, B., Comrie, A.C., Frakes, B., Brown, D.P., 2001: Developments and prospects in synoptic climatology. *Int. J. Climatol.*, 21, 1923–1950.

Zhang, X., et al., 2005: Trends in Middle East climate extreme indices from 1950 to 2003. *J. Geophys. Res.*, 110, D22104, doi:10.1029/2005JD006181.